

Influence of thermo-mechanical treatment on the superplastic behaviour of an AZ91 magnesium alloy

Z. Trojanová¹, Z. Száraz^{1*}, T. Ryspaev², V. Wesling²

¹*Department of Physics of Materials, Faculty of Mathematics and Physics, Charles University, Prague, Ke Karlovu 5, CZ-121 16 Prague 2, Czech Republic*

²*Institute of Welding Engineering and Cutting Manufacturing Processes (ISAF), Clausthal University of Technology, Agricola Str. 2, D-38678 Clausthal-Zellerfeld, Germany*

Received 28 May 2008, received in revised form 23 July 2008, accepted 28 July 2008

Abstract

Plastic deformation of magnesium alloy AZ91 was investigated at various strain rates in the interval from 3×10^{-5} to $1 \times 10^{-2} \text{ s}^{-1}$ and temperature of 420°C. Samples exhibiting superplastic behaviour were prepared by the three different thermo-mechanical treatments. Microstructure of samples was observed by the light microscopy. Strain rate sensitivity parameter m has been estimated by the abrupt strain rate change method. Possible physical mechanisms of the superplastic flow are discussed.

Key words: magnesium alloy, superplastic flow, dynamic recrystallization, grain boundary sliding, cavitation

1. Introduction

Low density, high specific strength and high damping capacity predestine magnesium alloys for use in structural applications and the transport industry. Considerable attention has been given to magnesium alloys in the last years [1–7]. However, magnesium alloys generally exhibit poor ductility and workability due to their hexagonal close-packed (HCP) structure with the shortage of crystallographic equivalent operating slip systems. For commercial cast Mg alloys the elongation to failure is usually less than 30–40 % even at elevated temperatures [8]. In order to increase chance for the structural applications of Mg alloys, the improvement of workability and development of plastic forming technology is required. These limitations may be significantly overcome by the finding out conditions for the superplastic flow of Mg alloys. The crucial problem is to develop the fine-grained alloy with low cost, low forming stress, low forming temperature and high forming rate. In order to reduce grain size, several processes have been used: severe plastic deformation, powder metallurgy techniques, rapid solidification or hot rolling. An alternative route to pre-

pare superplastic alloy is thermo-mechanical treatment. Cast materials are heat-treated in two stages and deformed by the hot extrusion. The grain structure can be refined via recrystallization in the alloy through overageing with a successive extrusion mechanical working. There is a limited knowledge about the characteristics and mechanisms of superplastic deformation of Mg alloys, which inhibit the spread of this forming process. Although superplastic behaviour of the AZ91 magnesium alloy has been observed by several authors [10–13], there is no satisfactory explanation of physical processes occurring during the superplastic flow.

In this paper the influence of the thermomechanical treatment on superplastic behaviour of the AZ91 magnesium alloy will be reported.

2. Experimental procedure

Composition of the alloy used in this study is introduced in Table 1. The as-received billets, produced from cast ingots were heat-treated in two stages. The first step was a solution treatment at 415°C for 10 h

*Corresponding author: tel.: +420 221911611; fax: +420 221911490; e-mail address: szaraz@karlov.mff.cuni.cz

Table 1. Chemical composition of the investigated AZ91 alloy in wt.%

Alloy	Mg	Al	Mn	Zn	Si	Cu	Fe
AZ91	bal.	9.0	0.4–0.7	0.5–0.9	0.05	0.025	0.004

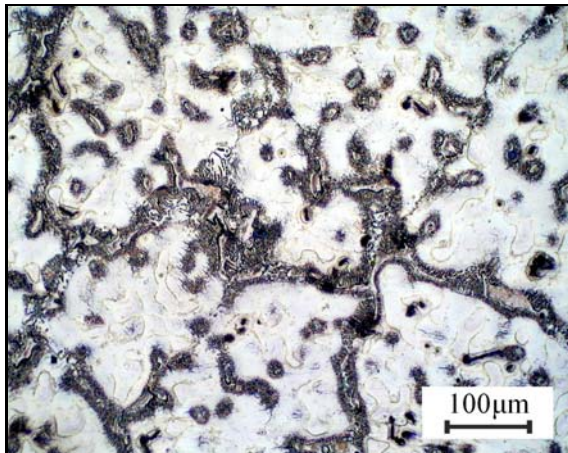


Fig. 1. Microstructure of the as-cast alloy with the typical dendritic structure.

following with the air quenching. Subsequently the billets were overaged at temperature in the range of 200–380 °C for 10 h. Finally the billets have been hot extruded at temperature of 350 °C to obtain rods.

Tensile specimens with a gauge length of 10 mm and gauge diameter of 6 mm were machined with a tensile axis parallel to the extrusion direction. Abrupt strain-rate jump tests in tension and tensile tests with a constant strain rate $\dot{\epsilon}$ were carried out using an Instron 5582 universal testing machine [14]. The deformation tests were carried out at the temperature of 420 °C. The furnace temperature was controlled with the accuracy of ± 1 °C.

The microstructure of the extruded alloys was observed by the light optical microscope Olympus. The grain structure was promoted by etching using HNO_3 solution in ethanol and acetic glycol solution.

3. Experimental results and discussion

Figure 1 shows the grain structure of the as-cast alloy with the typical dendritic structure. The material after homogenization was submitted in the second step, to the precipitation annealing at three temperatures: at 200 °C – AZ91-I, 300 °C – AZ91-II, 380 °C – AZ91-III. Resulting microstructures of the all three materials are introduced in Fig. 2a–c. Pictures were taken from the perpendicular section of samples (perpendicular to the extrusion direction). From these pic-

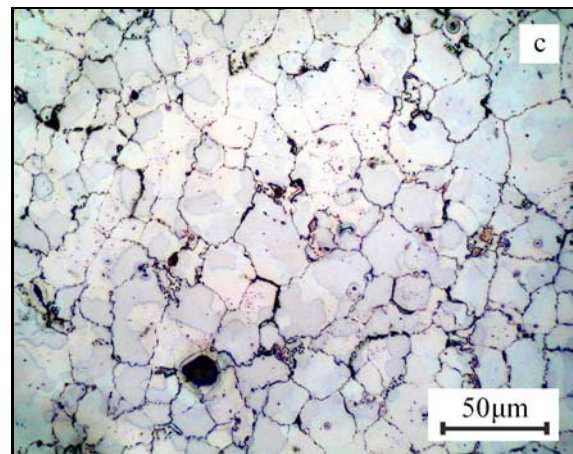
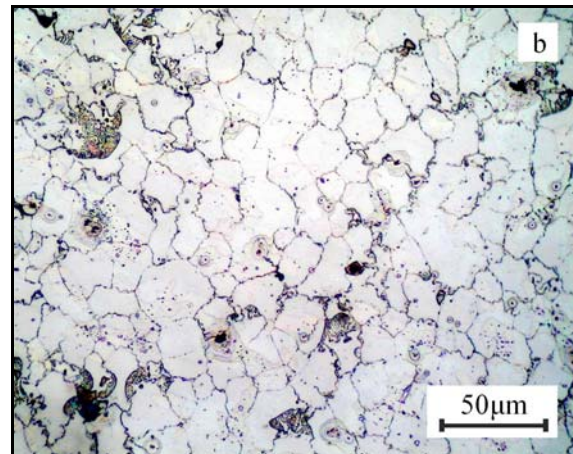
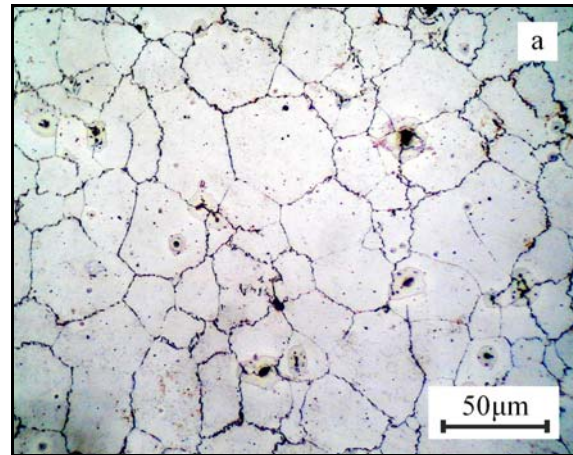
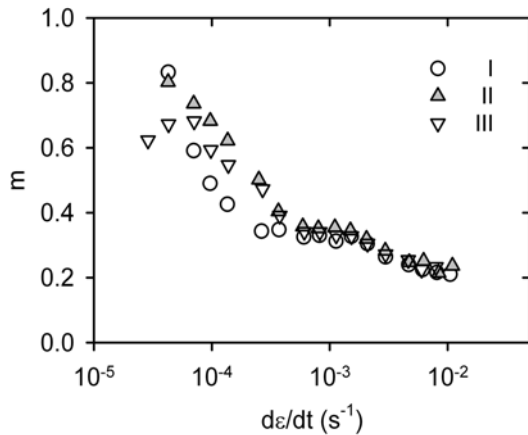
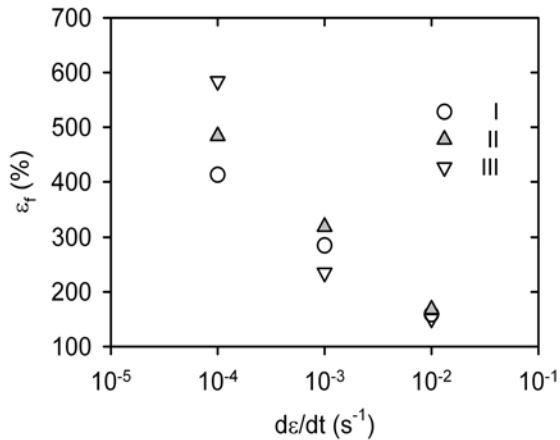


Fig. 2. Microstructure investigated after thermomechanical treating (section perpendicular to the extrusion direction): a) AZ91-I, b) AZ91-II, c) AZ91-III.

tures the grain sizes were estimated using special software (Lucie). The corresponding average grain sizes are introduced in Table 2. The extruded samples exhibit uniform grain structure; micrographs from the perpendicular sections of samples (parallel to the extrusion direction) show the same grain size and grain

Table 2. Grain size of the as-extruded alloys

Alloy	As-cast	AZ91-I	AZ91-II	AZ91-III
Grain size (μm)	100	17	10.5	11

Fig. 3. Strain-rate dependence of the parameter m of heat-treated and extruded samples at temperature of 420°C .Fig. 4. Strain-rate dependence of the elongation to failure estimated at 420°C .

shape. The grain refining depends on the temperature of the additional annealing in the second step.

High strain rate sensitivity of the flow stress is one of the main features of the superplastic deformation. High values of m and also the elongation to failure ε_f are observed only in a certain region of the strain rates and temperatures. Strain rate sensitivity parameter m , defined as $m = \left(\frac{d \ln \sigma}{d \ln \dot{\varepsilon}}\right)_T$ was measured by the abrupt strain rate change test. Values of the strain rate parameter m estimated for various strain rates and temperature of 420°C are introduced in Fig. 3. The strong strain rate dependence of the m -parameter is

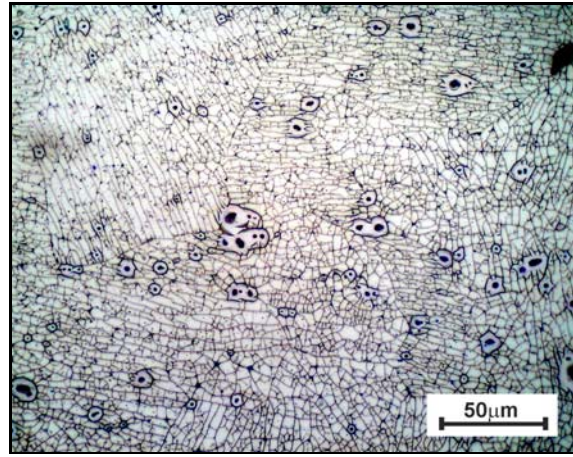


Fig. 5. Microstructure of the deformed AZ91-I sample in the cross-section.

obvious from the Fig. 3. Usually the m value of 0.3 is considered as a limit of the superplastic behaviour, i.e. only deformation at strain rates in the interval from 3×10^{-5} to $5 \times 10^{-3} \text{ s}^{-1}$ may be attributed to the superplastic deformation. It corresponds to results of deformation experiments. Elongation to failure ε_f depending on the strain rate is introduced in Fig. 4. For the AZ91-I samples the elongation to failure increases from 159 to 413 %, for AZ91-II 168 to 484 % and AZ91-III 154 to 584 %. Simultaneously a rapid decrease of the flow stress has been observed. Differences between samples aged at various temperatures (AZ91 I-III) are not significant. The elongation up to failure found for materials II and III is higher. It is very probably due to lower grain size.

Microstructure of the AZ91-I sample after high temperature deformation at the strain rate of $1 \times 10^{-4} \text{ s}^{-1}$ in the cross-section is introduced in Fig. 5. The network of very small grains ($\sim 1 \mu\text{m}$) is obvious from the picture. The old grain boundaries are in the picture still visible. The resulting grain size after deformation exhibits about $35 \mu\text{m}$. The inspection of the AZ91-II sample after deformation at 420°C showed in the direction parallel to the stress axis small cavities situated mainly on the grain boundaries (Fig. 6a). In the Fig. 6b taken in the vicinity of the fracture surface, coalescence of small cavities formed bigger damaged areas bounded by the original grain boundaries. The grain size increased also up to approximately $37 \mu\text{m}$. Figure 7a shows microstructure of the AZ91-III alloy from the perpendicular section after deformation at $1 \times 10^{-4} \text{ s}^{-1}$. The coarser grains originated from the initially fine dynamically recrystallized grains had grown as a result of high deformation temperature. Small cavities are visible among grains grown up to $40 \mu\text{m}$. Microstructure of the same sample from the parallel stress (extrusion) direction is introduced in Fig. 7b. Cavities

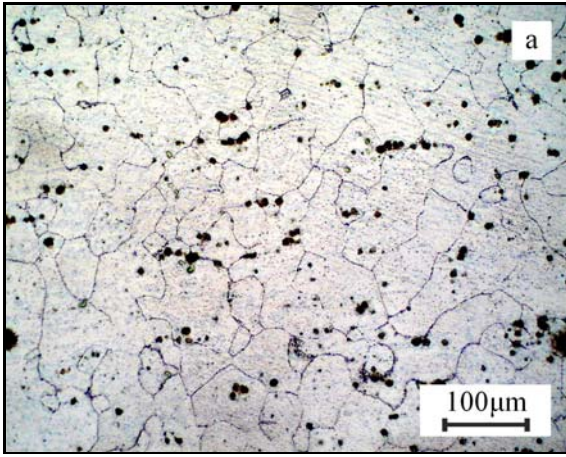


Fig. 6a. Formation of cavities in dynamic recrystallized grains (AZ91-II).

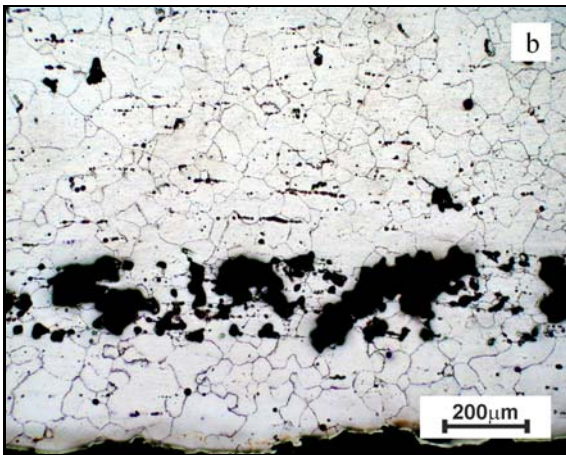


Fig. 6b. Coalescence of cavities in the vicinity of fracture surface (AZ91-II).

coalesced in the middle of the sample formed elongated hollow.

The superplastic deformation of the AZ91 alloy may be divided into three stages. In the first stage the small grains are deformed by the dislocation mechanism. Mori et al. [15] observed the microstructural evolution of the rolled AZ91 alloy. They detected no grain boundary sliding up to true strain of 0.1. Increasing dislocation density and subgrain formation is followed by dynamic recrystallization. Mabuchi and Higashi [16] found that the grain boundary diffusion rate is rather high, compared to that of Al. It is therefore suggested that dislocations which are piled up at (sub)grain boundaries are easily absorbed into (sub)grain boundaries and the recrystallization is accelerated. Small dynamically recrystallized grains visible in Fig. 5a are capable of grain boundary sliding [17]. Contribution of the grain boundary sliding increases with increasing strain. The grain bound-

ary sliding of fine recrystallized grains is accommodated by intergranular slip and grain boundary diffusion. Cavities formed at grain boundaries are obvious in Figs. 6a and 7a. Tan et al. [17] observed cavitations during superplastic deformation of AZ31 alloy. They observed filament formation between the recrystallized grains as a consequence of the diffusion of solute Zn atoms from the grain boundaries into filaments, therefore rendering the grain boundaries low in Zn content. In the next step the filaments between adjacent grains fractured and cavities were formed at grain boundaries. The nucleated cavities tend to coalesce with the neighbouring cavities. Subsequently, interlinkage of cavities will result in intergranular cracks and fracture.

The total strain ε_t at high temperature deformation can be expressed by

$$\varepsilon_t = \varepsilon_g + \varepsilon_{gbs} + \varepsilon_{dc}, \quad (1)$$

where ε_g is the strain due to slip inside of grains including the accommodating processes, ε_{gbs} is the strain resulted from the grain boundary sliding, ε_{dc} is the strain due to diffusion creep.

The superplastic flow in the AZ91 alloy is complex. At the beginning of the deformation process is realized by the dislocation glide. Increasing density of dislocations and their structuralization is followed by the recrystallization. Very small recrystallized grains are able of grain boundary sliding. Successive grain growth increases the grain size. The diffusion accommodation of the grain boundary sliding is more difficult which implies cavities formation. In various stages of deformation the percentage contribution of each mechanism, expressed in Eq. (1), is different. Different microstructure formed by three different samples preparation routes results in various superplastic behaviour. It is a consequence of the fact that the contributions of individual mechanisms to the total strain are different for each of the three types of samples.

4. Summary

Superplastic behaviour of the AZ91 magnesium alloy has been studied at 420°C in the strain rate interval from 3×10^{-5} to $1 \times 10^{-2} \text{ s}^{-1}$ for samples prepared by the thermo-mechanical treatment with the three different ageing temperatures. The highest elongation to failure was found for the samples prepared by the route III (precipitation ageing at 380°C). The superplasticity of the alloy has a complex character. The high strain to fracture is the result of several mechanisms: dislocation glide inside the grains, dynamic recrystallization, grain boundary sliding and diffusion processes.

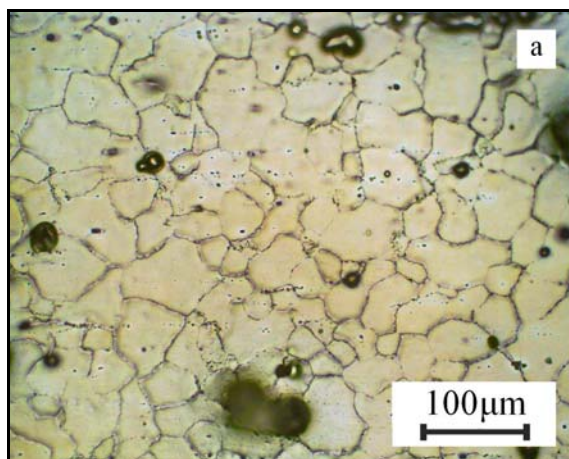


Fig. 7a. Microstructure of the AZ91-III sample from the perpendicular section to the stress axis.

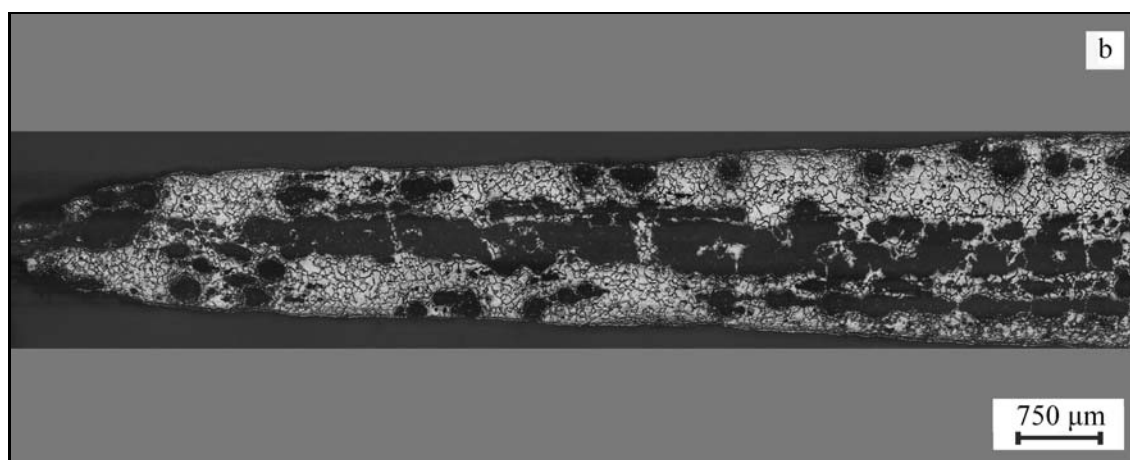


Fig. 7b. Picture from the same sample parallel to stress direction (in the vicinity of the fracture neck).

Acknowledgements

The authors dedicate this paper to Prof. Dr. Michael Boček on the occasion of his 80th birthday. This work is a part of the Research Project 1M 2560471601 “Eco-center for Applied Research of Non-ferrous Metals” that is financed by the Ministry of Education, Youth and Sports of the Czech Republic.

References

- [1] TROJANOVÁ, Z.—MILNERA, M.: *Kovove Mater.*, 44, 2006, p. 75.
- [2] LUKÁČ, P.—TROJANOVÁ, Z.: *Kovove Mater.*, 44, 2006, p. 243.
- [3] LUKÁČ, P.—KOCICH, R.—GREGER, M.—PADALKA, O.—SZÁRAZ, Z.: *Kovove Mater.*, 45, 2007, p. 115.
- [4] DOBRONĚ, P.—BOHLEN, J.—CHMELÍK, F.—LUKÁČ, P.—LETZIG, D.—KAINER, K. U.: *Kovove Mater.*, 45, 2007, p. 129.
- [5] BALÍK, J.—LUKÁČ, P.—BOHLEN, J.—KAINER, K. U.: *Kovove Mater.*, 45, 2007, p. 135.
- [6] KRÁL, R.—CHMELÍK, F.—KOULA, V.—RYDLO, M.—JANEČEK, M.: *Kovove Mater.*, 45, 2007, p. 159.
- [7] TROJANOVÁ, Z.—LUKÁČ, P.: *Kovove Mater.*, 45, 2007, p. 75.
- [8] ADVESIAN, M.—BAKER, H., Eds: *ASM specialty handbook Mg and Mg alloys*. Materials Park, Ohio, ASM International 1999.
- [9] SOLBERG, J. K.—TØRKLEP, J.—BAUGER, Ø.—GJESTLAND, H.: *Mater. Sci. Engn.*, A134, 1991, p. 1201.
- [10] MABUCHI, M.—IWASAKI, H.—YANASE, K.—HIGASHI, K.: *Scripta Mater.*, 36, 1997, p. 681.
- [11] MABUCHI, M.—AMEYAMA, K.—IWASAKI, H.—HIGASHI, K.: *Acta Mater.*, 47, 1999, p. 2047.
- [12] WEI, Y. H.—WANG, Q. D.—ZHU, Y. P.—ZHOU, H. T.—DING, W. J.—CHINO, Y.—MABUCHI, M.: *Mater. Sci. Engn.*, A360, 2003, p. 107.
- [13] WESLING, V.—RYSPEV, T.—SCHRAM, A.: *Mater. Sci. Engn.*, A462, 2007, p. 144.
- [14] BOOESHAGHI, F.—GARMESTANI, H.: *Scripta Mater.*, 40, 1999, p. 509.
- [15] MORI, T.—MABUCHI, M.—NAKAMURA, M.—ASAHINA, T.—IWASAKI, H.—AIZAWA, T.—HIGASHI, K.: *Mater. Sci. Engn.*, A290, 2000, p. 139.
- [16] MABUCHI, M.—HIGASHI, K.: *Acta Mater.*, 44, 1996, p. 4611.
- [17] TAN, J. C.—TAN, M. J.: *Mater. Sci. Engn.*, A339, 2003, p. 81.